# Kutatási jelentés a Csillagászati és Földtani Kutatóintézet (CSFK) által a Berger-barlangban 2022-ben végzett kutatási munkákról

Felelős kutatásvezető: Dr. Demény Attila, CSFK FGI igazgató

A mintázásokat végzi: Szilaj Rezső és Berentés Ágnes

A jelentést készítette: Berentés Ágnes és Dr. Demény Attila igazgató

2023. február 13.

Dr. Demény Attila
igazgató, az MTA rendes tagja

Bevezetés és rövid összefoglaló

A Balaton-felvidéki Nemzeti Park igazgatósága által 2022. január 11-én kiadott engedély (102-2/2022) alapján 2022. december 31-ig végeztünk kutatási tevékenységet a Berger-barlang járataiban. Az engedély alapján a 2022. február 17-én és 2022. július 18-án sikerült 4-4 résztvevővel mintavételezést végezni. A résztvevők: Berentés Ágnes, Szilaj Rezső (a barlang kutatásvezetője), Pulsfort Zsuzsanna, Borka Pál, Szabó Zoltán. A kutatási munka során víz és karbonát mintavételezés történt. Emellett 2022-ben a 2021-es mintavételezés során nyert minták feldolgozása, az adatok értelmezése történt meg.

2022-ben a barlangi munkák alapvetően a fizikokémiai paraméterek (hőmérséklet, pH, vezetőképesség, kémiai és stabilizotópos összetétel) meghatározását, valamint ehhez üveglemezek kihelyezését, júliusban a begyűjtését, az ezeken kiváló karbonát, valamint a benyújtott tervekben megadott és begyűjtött karbonát minták elemzését célozták. A 2022-ben kapott eredményekből 1 kézirat elkészült, a Quaternary Research folyóirat jelenleg bírálja. A kéziratot a jelentéshez csatoltuk, a Nemzeti Park engedélyére és részvételére hivatkoztunk mind a szövegben, mind a köszönetnyilvánítás fejezetében.

Az ásványtani/ geokémiai elemzések mellett a korábbi mikrobiológiai mintavételezéskor beszerzett minták DNS elemzése történt meg külföldi laboratóriumban. Az eredmények publikálása folyamatban van.

Tartalom:

A jelentés a következőket tartalmazza:

1) Terepi dokumentáció a 2022. február 17-i barlangi munkáról

2) Terepi dokumentáció a 2022. július 18-i barlangi munkáról

3) A mikrobiológiai kutatás eredményei

4) „Subaqueous carbonate speleothems as paleotemperature archives– comparison of clumped isotope and inclusion-based formation temperature determinations" – kézirat beküldve a Quaternary Research folyóirathoz

1) Berger Károly-barlang

Titkok-tava és Nagy Lángos két tavának víz és karbonát mintázása

Mintagyűjtés ideje: 2022_02_17

Mintázást végezte: Berentés Ágnes

Mintázásnál jelen voltak: Szilaj Rezső, Pulsfort Zsuzsanna, Szabó Zoltán

A Berger Károly barlang ezúttal két védett tavához, a Titkok-tavához és a Nagy Lángoshoz tértünk vissza. A víz és levegő paraméterei mellett karbonátkiválásokat is gyűjtöttünk a tavak környékéről, valamint a karbonátképződés intenzitásának vizsgálata végett tavanként 5-5 üveglapot is kihelyeztünk, melyek egy része a víztükör alá került és sorba helyezve őket, 1-2 üveglap a víz szintje felé is esik.
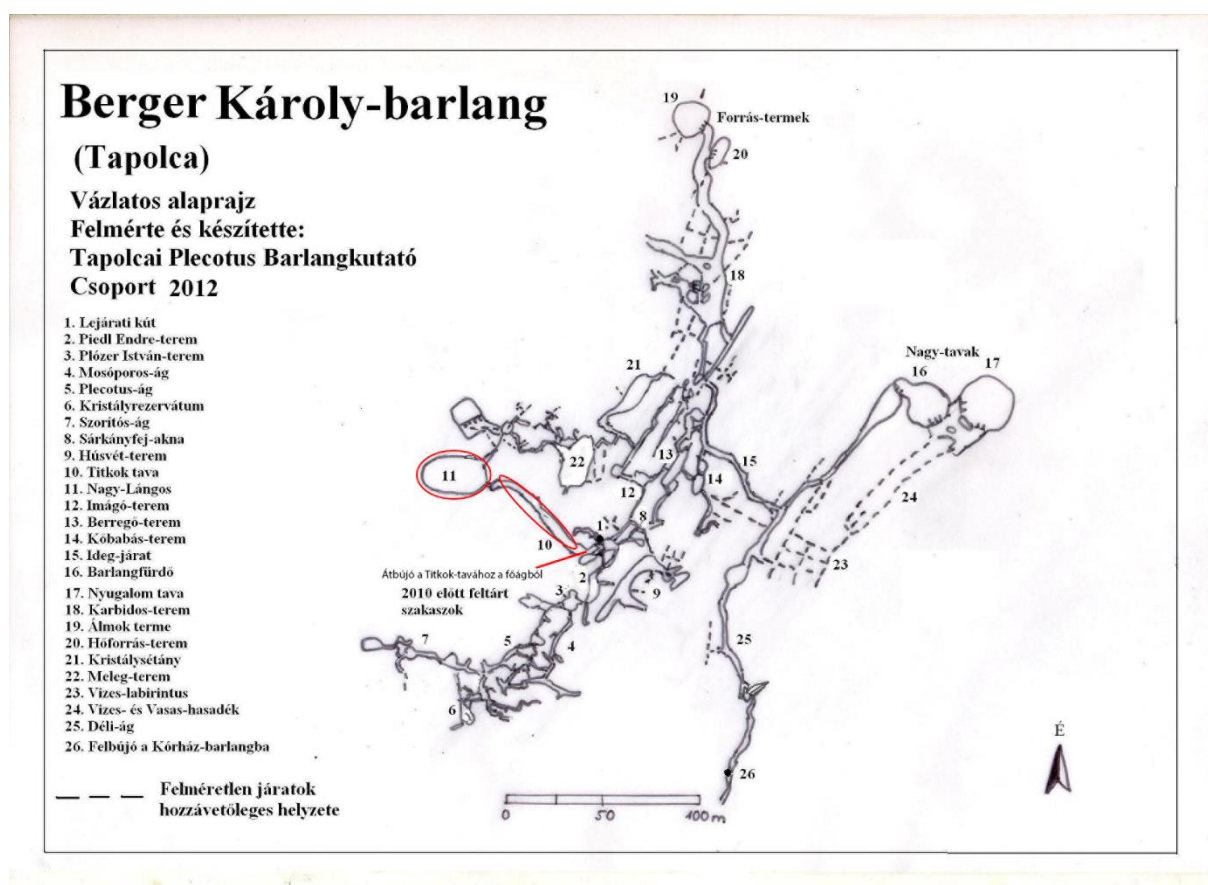
Mintázott területek.

	pH	^{0}C	vez.kép (μS/cm)	CO_2 (tf.%)	Mintaszámok	Egyéb mintázások
Bejáratban mért értékek	–	17,1	–	1,02		
Titkok-tava	7,569	19	943	0,77	Bg_Titkok-tava_01	stabilizotóp +nyomelem +titrálás
Nagy Lángos 2-es tó	–	23,3	901	0,82	Bg_NL/2_01	stabilizotóp +nyomelem +titrálás
Nagy lángos 1-es tó	–	24,3	919	0,82	Bg_NL/1_02	stabilizotóp +nyomelem +titrálás

1. táblázat: A mintázott tavak paraméterei. A pH mérő elektróda a vízen való átkelés vagy a hideg műszerre lecsapódó pára folytán nedves lett, a Nagy Lángosok pH értékeire hibás (savas) értéket adott. A Nagy Lángos tavai a számozás szerint a Titkok-tava felől a 2-es, a kerülőút felől érkezve az első kapta az 1-es számot.

Üveglap számozása	Mintavételezés helyszíne	tiszta üveglap súlya (g)	kihelyezés időpontja	Megjegyzés
1	Titkok-tava	8,0309	2022_02_17	
2	Titkok-tava	8,1101	2022_02_17	
3	Titkok-tava	8,0227	2022_02_17	
4	Titkok-tava	8,1929	2022_02_17	
5	Titkok-tava	8,0331	2022_02_17	
6	Nagy Lángos 2. tó	8,3043	2022_02_17	
7	Nagy Lángos 2. tó	8,2828	2022_02_17	
8	Nagy Lángos 2. tó	8,2735	2022_02_17	
9	Nagy Lángos 2. tó	8,2644	2022_02_17	
10	Nagy Lángos 2. tó	8,2986	2022_02_17	
11	Nagy Lángos 1. tó	8,1362	2022_02_17	A 2-es tóhoz közelebb eső részre helyezve

12	Nagy Lángos 1. tó	8,1860	2022_02_17	A 2-es tóhoz közelebb eső részre helyezve
13	Nagy Lángos 1. tó	8,0541	2022_02_17	A 2-es tóhoz közelebb eső részre helyezve
14	Nagy Lángos 1. tó	8,1203	2022_02_17	A 2-es tóhoz közelebb eső részre helyezve
15	Nagy Lángos 1. tó	8,3118	2022_02_17	A 2-es tóhoz közelebb eső részre helyezve
16	Nagy Lángos 1. tó	7,9043	2022_02_17	A raftosabb részébe helyezve a tónak
17	Nagy Lángos 1. tó	7,7091	2022_02_17	A raftosabb részébe helyezve a tónak
18	Nagy Lángos 1. tó	8,1530	2022_02_17	A raftosabb részébe helyezve a tónak
19	Nagy Lángos 1. tó	7,8693	2022_02_17	A raftosabb részébe helyezve a tónak
20	Nagy Lángos 1. tó	8,2655	2022_02_17	A raftosabb részébe helyezve a tónak

2. táblázat. A tavakba kihelyezett üveglapok helye és súlya.

5 db üveglap a Nagy Lángos 2-es tavában (1,5 db ér a víz szintje fölé, 6-10-ig, lentről felfelé számozott üveglapok kerültek ide).

Nagy Lángos 1-es tava, bal középső részén az üveglapokkal.

	mintaszám	helyszín	egyéb	begyűjtés időpontja
1	Bg_2022.02.17_01	Titkok-tava felé menet, a főágból átbújás után		2022_02_17
2	Bg_2022.02.17_02_asv.	Titkok-tava, víz feletti kivállás		2022_02_17
3	Bg_NL/2_kalc/01	Nagy Lángos 2. tava		2022_02_17
4	Bg_NL/2_02/kalc.	Nagy Lángos 2. tava	vízszint alatti kis karbonátcsomó	2022_02_17
5	Bg_NL/2_03/kalc.	Nagy Lángos 2. tava	plafonképződmény	2022_02_17
6	Bg_NL/1_02_asv/02	Nagy Lángos 2. tava	Medenceujj törmelékből	2022_02_17
7	Bg_NL/1_02_asv/03	Nagy Lángos 1. tava	Aragonitos jellegű, ágas-bogas minta a plafonról	2022_02_17
8	Bg_NL/1_ásv/05	Nagy Lángos 1. tava	Medenceujj a törmelékből	2022_02_17
9	Bg_NL/1_ásv/06	Nagy Lángos 1. tava	aragonitos jellegű törmelék	2022_02_17

3. táblázat: a begyűjtött képződmények mintalistája.

Bg_NL/2_kalc/01

Bg_NL/2_02/kalc. minta: Nagy Lángos 2 tavának vize alól.

Bg_NL/1_02_asv/02 minta: medenceujj törmelékből, a két Lángos közül

Bg_NL/1_ásv/05 minta: Nagy Lángos 1 tava mellől törmelékből

Bg_NL/1_ásv/06 minta: Nagy Lángos 1 tava mellől, törmelékből

2) Berger Károly-barlang

Titkok-tava és Nagy Lángos két tavának vízmintázása, üveglemezek begyűjtése és kihelyezése

Mintagyűjtés ideje: 2022_07_18

Mintázást végezte: Berentés Ágnes

Mintázásnál jelen voltak: Szilaj Rezső, Pulsfort Zsuzsanna, Borka Pál,

A 2022 februárjában kihelyezett üveglapok begyűjtése volt a cél a három tó partjáról, valamint az ehhez kapcsolódó vízmintavételezések pH, vez.kép és vízhőmérséklet-mérés.

Az üveglemezek begyűjtése mellett a hosszú távú karbonátkiválási folyamat vizsgálatára a kitűzött helyekre újabb üveglemezek kerültek.

	pH	^{0}C	vez.kép (μS/cm)	Mintaszámok	Egyéb mintázások
Titkok-tava	7,337	19,0	1022	Bg_Titkok-tava_01/03	stabilizotóp +nyomelem +titrálás +Ba(OH)2
Nagy Lángos 2-es tó	7,383	22,8	951	Bg_NL/2_02	stabilizotóp +nyomelem +titrálás +Ba(OH)2
Nagy lángos 1-es tó	7,408	24,3	982	Bg_NL/1_02	stabilizotóp +nyomelem +Ba(OH)2

4. táblázat. A tavakból gyűjtött vízminták és elvégzett mérések.

Titkok-tavába helyezett üveglapok begyűjtés előtt (1-5-ig)

A Nagy-lángos 2-es tavába helyezett üveglapok begyűjtés előtt (5-10-ig).

A Nagy-lángos 1-es tavába helyezett üveglapok begyűjtés előtt (16-20-ig)

4) A mikrobiológiai kutatás eredményei
Lange-Enyedi Nóra Tünde, Makk Judit

A barlangban ezidáig nem történt vizsgálat a mikrobiális diverzitás széleskörű feltárására. A baktériumközösségek biogeokémiai folyamatokban való részvételét szeretnénk tanulmányozni. Célunk a Berger Károly-barlangban a mikrobiális tevékenység és a karbonátképződés összefüggéseinek feltárása, amit korábbi, 10 °C-os léghőmérsékletű epigén barlangi kutatások során sikerült kimutatni (Enyedi et al., 2020). Azokhoz képest a barlang a regionális áramlási rendszerekből származó vizek és a meteorikus vizek a keveredési korrózió hatására alakult ki a város alatt 12-15 méter mélyen (Móga és mtsai, 2013). A tavak hőmérséklete 20-30 °C, a barlang levegője is melegebb (13-16,5 °C) a hazai barlangi viszonyokhoz képest és a felszín alatti vizek fejlődésének megfelelően magasabb szulfát- és klorid-koncentrációval jellemezhetőek (Szilaj, 2006; 2011).

Eredmények

A 2020. szeptember 5-én, október 1-jén és 26-án történő mintavétel során vett minták feldolgozása történt meg ezidáig. A mintákat Berentés Ágnestől kaptuk meg, melyek a kiválások felületéről származó kenetminták és barlangi talajminták az Álmok-terméből, a Hőforrás-teremből (Babahasadék), a Húsvét-teremből, az Imágó-teremből és a Nagy-tavak környékéről származtak. Kaptunk kenetmintát logomitok melletti területről a Zúzda után, illetve vízmintákat a Meleg-terem után, az 1. számú Nagy-tóból, az Álmok-terméből, a Hasadék-terem savas és nem savas tavakból, valamint feltehetően vas-oxidos mintát a Nagy-tavak előtti területről.

A bakteriális közösség elemzését a mintákból kivont közösségi DNS 16S rRNS-gén V3-V4 régiójának új-generációs bázissorrend meghatározásával (Illumina MiSeq platformon, Michigan State University) végeztük (Tóth et al., 2020). A bioinformatikai kiértékelés (mothur v1.44.3) az ELKH ATK martonvásári szerverén történt, melynek során minőségi szűrést végeztünk, kiszűrtük az amplifikációs és szekvenálási hibákat, a kiméra szekvenciákat és a szingleton szekvenciákat (Schloss et al., 2009). A szekvenciák illesztése az SILVA Release138 SSU NR referencia adatbázis segítségével történt (Quast et al., 2013). Az OTU-k (operatív taxonómiai egységek) megállapítása 97%-os szekvencia hasonlósági küszöbnél történt (Tindall et al., 2010). A sikeresen megvizsgált mintákat tartalmazza az 5. *táblázat*.

5. táblázat: A Berger-barlangból (BG) 2020-ban mikrobiológiai vizsgálatok céljára vett minták.

Mintaszám	Minta jelzés	Helyszín	Minta	Gyűjtés ideje	°C	pH	Vez.kép.
Bg_Al_01	BGAC	Álmok-terme	kalcittűk környékéről kenet	2020.09.05	27,2	7,377	953
Bg_Al_02	BGAW	Álmok-terme tó	víz	2020.10.26			
Bg_Sav_01	BGBS	Babahasadék, savas tava	homokos talaj	2020.09.05	31,4	6,7	nincs adat
	BGBC	Babahasadék, savas tava	vízközeli visszaoldott felületről kenet	2020.09.05			
Bg_Sav_02	BGBW	Babahasadék, savas tava	víz	2020.10.26			
Bg_NS_02	BGBNW	Babahasadék nem savas tava	víz	2020.10.26			
Bg_NS_CS_01	BGBNC2	Babahasadék nem savas tava	cseppkőről mikrobi. kenet.	2020.10.26			
Bg_H1_01	BGHS	Húsvét-terem	homokos talaj	2020.09.05	18,8	7,18	875
	BGHC	Húsvét-terem	kalcittűk környékéről kenet	2020.09.05			
Imago_01	BGIR	Imágó-terem	karbonátosodott gyökerek és kalcitlemezek	2020.09.05	x	x	x
Bg_Log_01	BGL	Logomitok a Zúzda után	logomitokról felületi kenetminta	2020.09.05	x	x	x
Bg_Cl_01	BGCW	Meleg-terem után	víz	2020.10.01	18,8	7,22	579
	BGC	Meleg-terem után	kalcit kenet	2020.10.01			
Bg_g_01	BGG	Nagy tavak előtt	vas-oxidos darabka	2020.10.01	x	x	x
Bg_Nt_01	BGNW	1.sz. Nagy-tó	víz	2020.10.01	21,1	7,178	974
	BGNS	1.sz. Nagy-tó	talaj	2020.10.01			

A különböző minták baktériumközösségének elemzése során kapott eredmények mennyiségi jellemzőit a *6. táblázat* foglalja össze.

6. táblázat: A 16S rRNS-gén amplikon szekvenálással kapott bakteriális OTU számok és diverzitás indexek. Az indexek esetében ábrázolt értékek az adathalmaz újramintavételezésének átlagértékei 15684 (Bacteria) és 5824 (Archaea) szekvencia alapján. A lefedettség értékek a Good-féle lefedettség becslő index alapján lettek számítva.

Minta	Csoport	Szekvenciaszám	OTU-szám	Lefedettség (%)	Shannon-index	Inverz Simpson index (1/D)
BGAC	Bacteria	32939	590	100,00%	2,44	4,72
BGAW	Bacteria	22037	1104	100,00%	4,29	20,98
	Archaea	5824	107	99,98%	3,26	13,4
BGBC	Bacteria	22170	777	99,99%	4,45	29,01
	Archaea	21358	152	100,00%	2,36	4,16
BGBNC2	Bacteria	43285	545	100,00%	3,22	13,04
BGBNW	Bacteria	45855	472	100,00%	3,86	9,90
BGBS	Bacteria	24384	575	100,00%	3,28	6,11
	Archaea	23141	225	100,00%	3,22	14,5
BGBW	Bacteria	35025	109	100,00%	1,94	3,57
BGC	Bacteria	29979	492	100,00%	2,29	2,93
	Archaea	19176	89	100,00%	2,28	5,78

BGCW	Bacteria	29795	1148	100,00%	5,43	42,39
BGG	Bacteria	17470	477	100,00%	4,50	36,29
	Archaea	28094	118	100,00%	2,56	7,53
BGHC	Bacteria	36797	466	99,99%	2,10	3,65
	Archaea	32946	127	99,99%	2,51	6,98
BGHS	Bacteria	35809	1140	100,00%	5,57	87,50
BGIR	Bacteria	24675	566	100,00%	3,31	7,96
	Archaea	22776	177	100,00%	2,45	5,35
BGL	Bacteria	62876	1119	100,00%	2,91	6,39
BGNS	Bacteria	15684	536	100,00%	4,74	41,41
	Archaea	28527	176	100,00%	2,90	9,93
BGNW	Bacteria	22025	363	100,00%	2,50	4,77
	Archaea	15815	188	99,98%	1,62	2,74

6.táblázat folytatása

Az eredmények alapján a szekvenciák száma a Bacteria doménben megfelelő lefedettséget adott a bakteriális diverzitás feltárásához az ősbaktériumokkal szemben, melyekből esetenként elhanyagolható mennyiségű szekvenciát tudtunk kimutatni. A minták diverzitása változatosan alakult, a különböző minták diverzitása nem volt hasonló a Bacteria és az Archaea doménben (*6. táblázat*).

A Bacteria doménbe tartozó baktériumközösségek jelentősen különböztek más hazai epigén karsztbarlangok baktériumközösségeitől, mely feltételezhetően a barlang mélységéből, hőmérsékletéből és a részleges hévízi eredetből adódhat (*1. ábra*). A mintákban főként a Proteobacteria törzs tagjai voltak jelen a legnagyobb mennyiségben. Őket követték abundanciában az Actinobacteria törzs tagjai, melyek főként a logomit felületén (BGL) alkották jelentős hányadát a baktériumközösségnek, illetve a Firmicutes különösen a kalcitos minták felületén volt nagy mennyiségben (BGL, BGAC, BGBC). A vas-oxidos minta (BGG) jelentős mértékben különbözött a többi mintától, nagyszámú Myxococcota és Methylomirabilota törzsekbe tartozó szekvenciával. Az egymáshoz közelebbi mintavételi helyek baktériumközösségei mutattak hasonlóságot.
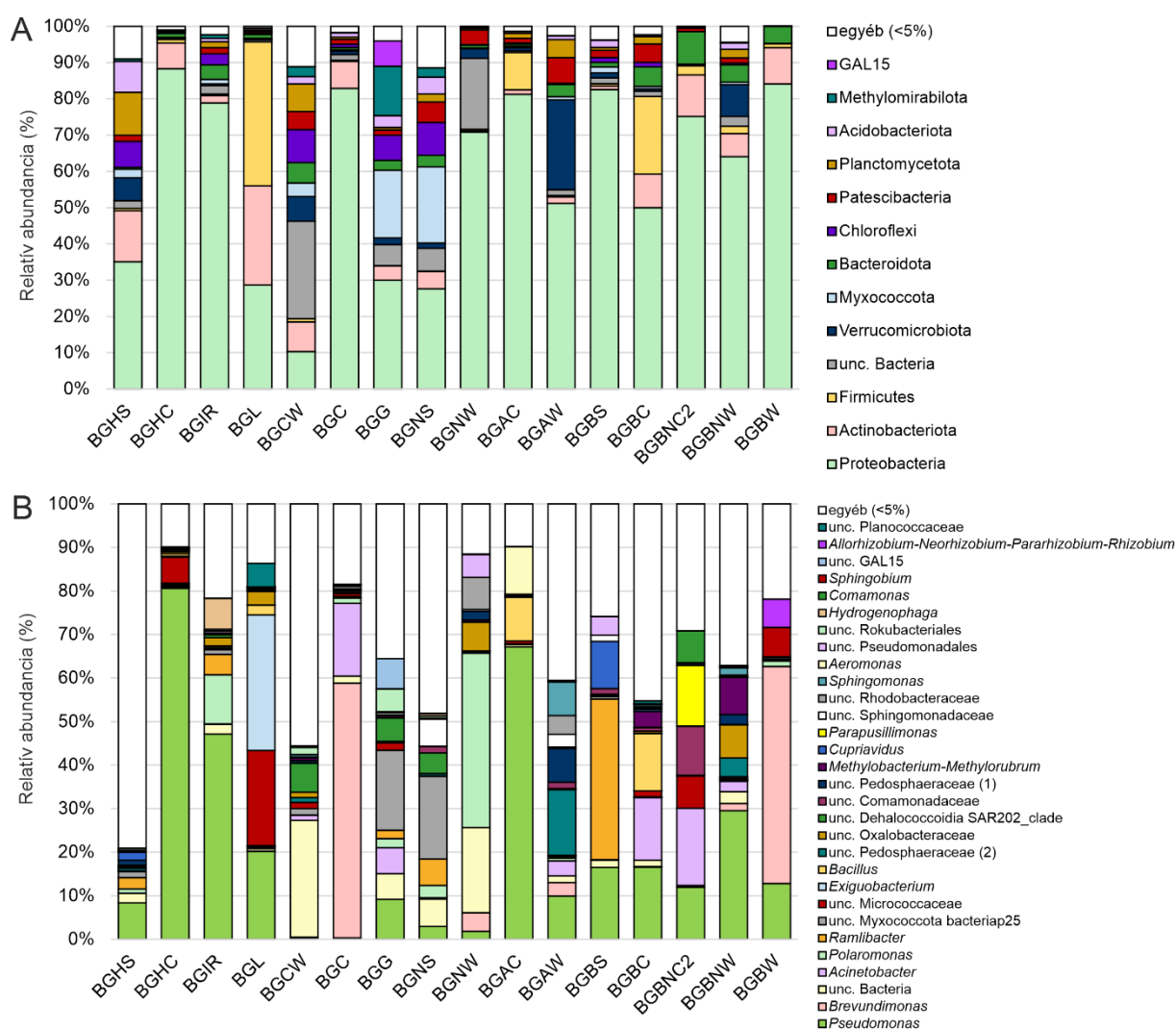
1. ábra: A Berger Károly-barlangból 16S rRNS-gén újgenerációs amplikon szekvenálással kimutatott baktériumközösségek megoszlása a minták között A) törzs, B) nemzetség szinten. Jelmagyarázat: unc. (uncultured) – azonosítatlan.

A barlangi minták mélységi eredetüknek megfelelően nagy mennyiségű, a tudomány számára még ismeretlen baktériumcsoport jelenlétéről is tanúskodtak. Számos OTU ismeretlen nemzetség vagy magasabb rendszertani kategória képviselője, különösen az Archaea doménen belül (*2. ábra*), a Bacteria doménen belül a vízmintákban (BGCW, BGNW; *1. ábra*). A legtöbb azonosított Bacteria doménbe tartozó nemzetség ismert képviselői aerob kemoorgano-heterotróf, köztük komplex szerves anyagok (kitin, cellulóz, lignin) lebontására képes baktériumok, pl. *Pseudomonas* és *Acinetobacter* spp. tagjai egymáshoz képest fordított abundanciával. Számos kalcium-karbonát kiválasztására potenciálisan képes baktériumot sikerült kimutatni (pl. *Pseudomonas, Bacillus, Acinetobacter, Pseudarthrobacter, Exiguobacterium, Cupriavidus* spp.), valamint a BGBS mintában nagyobb számban intracelluláris kalcium-foszfát precipitációra is képes *Ramlibacter* nemzetség

közel rokonait (Benzerara et al., 2004). A barlangokban gyakran előforduló, viszonylag alacsony szerves anyag tartalom miatt megjelenő oligotróf (pl. *Brevundimonas* sp.), kemolitotróf autotróf baktériumok (pl. *Hydrogenophaga* sp., *1. ábra*) és ammónia-oxidáló ősbaktériumok (Crenarchaeota törzs: *Nitrosarchaeum* sp., *Candidatus* Nitrososphaera, *Candidatus* Nitrosotalea, *Candidatus* Nitrosotenuis) is jelen vannak (*2. ábra*), melyek képesek lehetnek a barlangi környezetben szén- és nitrogén-körforgalom fenntartására és a biofilmek alapját képezhetik.
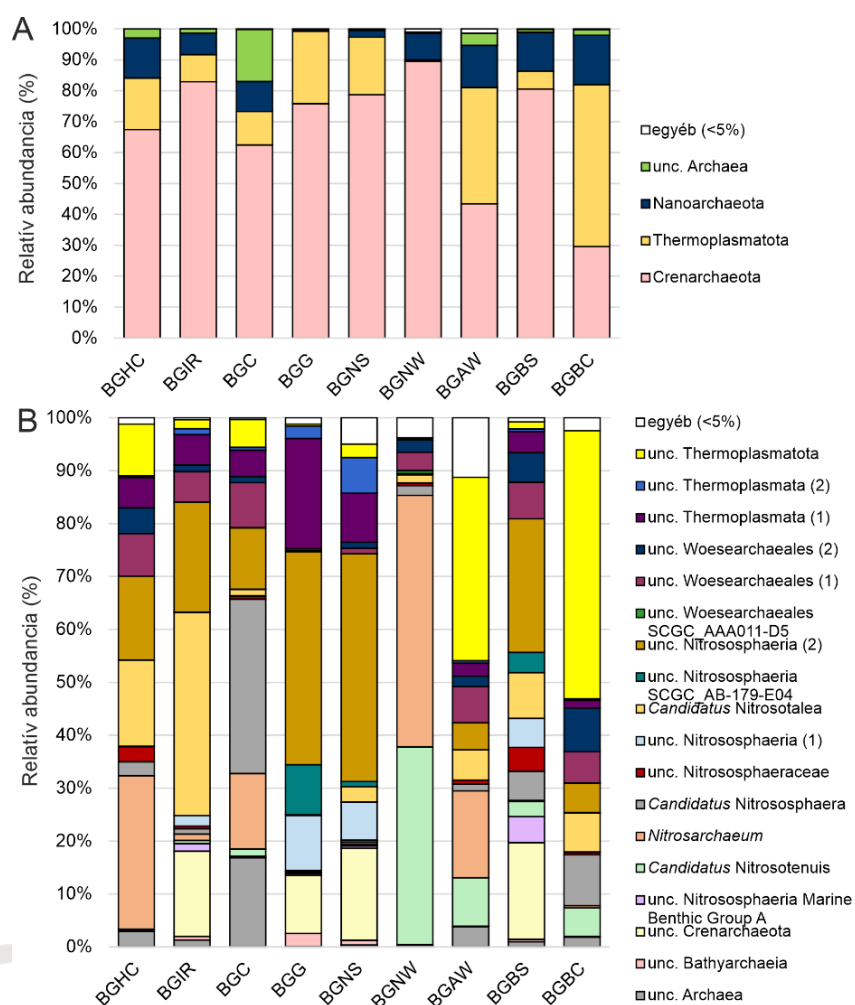
2. ábra: A Berger Károly-barlangból 16S rRNS-gén újgenerációs amplikon szekvenálással kimutatott ősbaktérium közösségek megoszlása a minták között A) törzs, B) nemzetség szinten.
Jelmagyarázat: unc. (uncultured) – azonosítatlan.

Irodalomjegyzék

Benzerara, K., Menguy, N., Guyot, F., Skouri, F., de Luca, G., Barakat, M., Heulin, T. (2004). Biologically controlled precipitation of calcium phosphate by *Ramlibacter tataouinensis*. *Earth and Planetary Science Letters*, *228*(3-4), 439–449.

Enyedi, N. T., Makk, J., Kótai, L., Berényi, B., Klébert, S., Sebestyén, Z., Molnár, Z., Borsodi, A. K., Leél-Őssy, S., Demény, A., Németh, P. (2020). Cave bacteria-induced amorphous calcium carbonate formation. *Scientific Reports*, *10*(1), 1–12.

Móga, J., Kiss, K., Szabó, M., Borsodi, A. K., Kéri, A., Mari, L., Knáb, M., Iván, V. (2013). Hazards and landscape changes (degradations) on Hungarian karst mountains due to natural and human effects. *Journal of Mountain Science*, *10*(1), 16–28.

Quast, C., Pruesse, E., Yilmaz, P., Gerken, J., Schweer, T., Yarza, P., Peplies, J., Glöckner, F. O. (2013). The SILVA ribosomal RNA gene database project: Improved data processing and web-based tools. *Nucleic Acids Research*, *41*(D1), 590–596.

Schloss, P. D., Westcott, S. L., Ryabin, T., Hall, J. R., Hartmann, M., Hollister, E. B., Lesniewski, R. A., Oakley, B. B., Parks, D. H., Robinson, C. J., Sahl, J. W., Stres, B., Thallinger, G. G., Van Horn, D. J., Weber, C. F. (2009). Introducing mothur: Open-source, platform-independent, community-supported software for describing and comparing microbial communities. *Applied and Environmental Microbiology*, *75*(23), 7537–7541.

Szilaj R. A tapolcai Plecotus Barlangkutató Csoport 2006. évi beszámolója.

Szilaj R. A tapolcai Plecotus Barlangkutató Csoport 2011. évi beszámolója.

Tindall, B. J., Rosselló-Móra, R., Busse, H. J., Ludwig, W., Kämpfer, P. (2010). Notes on the characterization of prokaryote strains for taxonomic purposes. *International Journal of Systematic and Evolutionary Microbiology*, *60*(1), 249–266.

Tóth, E., Toumi, M., Farkas, R., Takáts, K., Somodi, C., Ács. É. (2020). Insight into the hidden bacterial diversity of Lake Balaton, Hungary. *Biologia Futura*, *70,* 383–391.

1   **Subaqueous carbonate speleothems as paleotemperature archives – comparison of**

2   **clumped isotope and inclusion-based formation temperature determinations**

3   Attila Demény[1,2], Ágnes Berentés[1,2], László Rinyu[3], Ivett Kovács[1,2], Gergely Surányi[4],

4   Magdolna Virág[5]

5   [1] Institute for Geological and Geochemical Research, Research Centre for Astronomy and
6   Earth Sciences, ELKH, Budapest, Budaörsi út 45, H-1112, Hungary

7   [2] CSFK, MTA Centre of Excellence, Budapest, Konkoly Thege Miklós út 15-17., H-1121,
8   Hungary

9   [3] Institute for Nuclear Research, Isotope Climatology and Environmental Research Centre,
10   Debrecen, Bem tér 18/C, H- 4026, Hungary

11   [4] Institute for Particle and Nuclear Physics, Wigner Research Centre for Physics, Budapest,
12   Konkoly-Thege Miklós út 29-33., H-1121, Hungary

13   [5] Department of Physical and Applied Geology, Eötvös Loránd University, Pázmány Péter
14   sétány 1/C., Budapest, H-1117, Hungary

15

16   **Abstract**

17   Clumped isotope measurements of carbonates and stable isotope analyses of water trapped

18   in fluid inclusions are both promising techniques to determine carbonate formation

19   temperatures. Cave-hosted carbonate deposits (speleothems) would be excellent targets for

20   such studies, but kinetic fractionations and diagenetic influences frequently deteriorate the

21   temperature data obtained with these methods. However, subaqueous carbonate deposits

22   may provide reliable data as kinetic fractionations are less significant in underwater

23   environment. In the present study subaqueous carbonate formations were investigated,

24   whose formation temperatures were i) directly measured in the water, or ii) calculated using

25   host carbonate and inclusion water compositions. We have also investigated the effect of

26   sample preheating conditions to provide the most reliable inclusion water compositions. Our

27 study shows that subaqueous carbonate speleothems are useful targets for clumped isotope

28 and inclusion water analyses, and therefore they are valuable paleotemperature archives.

29 **Keywords**: subaqueous carbonate, speleothem, clumped isotope composition, stable

30 isotope compositions, fluid inclusion, formation temperature

31

32 **Introduction**

33 Carbonate speleothems (called speleothems from here for the sake of simplicity) are

34 attractive subjects of paleoclimate research as they can be dated with absolute dating

35 methods, they are formed in closed cave environments that prevents them from significant

36 late-stage alteration, and they provide various proxy data from which past climate

37 conditions can be deciphered (see the comprehensive review by Fairchild and Baker, 2012).

38 The age and proxy datasets are used to determine changes in temperature, humidity,

39 precipitation amount, seasonal variations, moisture transport routes, and even

40 meteorological teleconnections (e.g., Lachniet, 2009). On the other hand, quantitative

41 determination of climate conditions are rather difficult as the proxy data are usually not well

42 calibrated with respect to meteorological parameters, and the validity of recent calibrations

43 in the geological past is questionable. A typical example is stable oxygen isotope composition

44 ($\delta^{18}O$) of speleothems, which is basically determined by the formation temperature and

45 water composition together (e.g., O'Neil et al., 1969; Coplen, 2007; Tremaine et al., 2011),

46 and hence water composition should be known to calculate formation temperature. A

47 solution may be provided by the direct measurement of water composition by extracting

48 inclusion-hosted H_2O and its $\delta^{18}O$ determination. Conventionally the $^{18}O/^{16}O$ ratios were

49 analysed in the extracted H_2O by mass spectrometry that required CO_2-H_2O equilibration in

50   micro-sealed vessels (Socki et al., 1999) or reaction of H_2O with fluorine compounds (O'Neil

51   and Epstein, 1966) in case of speleothem-hosted inclusion waters (Yonge, 1982). These

52   methods are rather complicated or dangerous, hence the new techniques of using a high-

53   temperature conversion elemental analyzer attached to a mass spectrometer, or the

54   application of laser spectroscopy – that allows direct and combined determination of $^2H/^1H$

55   and $^{18}O/^{16}O$ ratios in H_2O vapor – induced a revolution in fluid inclusion stable isotope

56   analyses (Vonhof et al., 2006; Dublyansky and Spötl, 2009; Arienzo et al., 2013; Affolter et

57   al., 2014). With both of the $\delta^{18}O_{water}$ and $\delta^{18}O_{carbonate}$ values in hand and with the knowledge

58   of the temperature dependence of calcite-water oxygen isotope fractionation in

59   speleothems (Coplen, 2007; Demény et al., 2010; Tremaine et al., 2011; Johnston et al.,

60   2013; Daëron et al., 2019), the formation temperature might be calculated. However,

61   although some speleothems yielded reliable temperature data, some studies have dealt

62   with only δ^2H values, owing to diagenetic alterations that changed the original oxygen

63   isotope compositions in the inclusion-hosted water (Demény et al., 2016; 2021; Affolter et

64   al., 2019).

65   With the invention of clumped isotope analyses and the discovery of temperature

66   dependence of preferential bonding („clumping") of ^{13}C and ^{18}O (Ghosh et al., 2006), direct

67   determination of carbonate formation temperature without the need of water composition

68   became possible. Experimental (e.g., Jautzy et al., 2020), empirical (e.g., Kele et al., 2015),

69   and combined (Anderson et al., 2021) calibrations of temperature dependence of clumped

70   isotope compositions (Δ_{47} values, the deviation of actual abundance of $^{13}C^{18}O^{16}O$ from the

71   thermodynamically determined stochastic distribution, Eiler, 2007) provide equations to

72   calculate paleotemperature simply using measurements of Δ_{47} values. However,

73   speleothems rarely yielded reliable formation temperatures (e.g., Meckler et al., 2015; Duan

74   et al., 2022) due to kinetic fractionations along the karstic water migration routes, on the

75   stalagtite surfaces, and finally on the drip water arrival point on the stalagmite tips

76   (Deininger et al., 2021). Nevertheless, speleothems that formed at very low growth rate (i.e.,

77   reaching dynamic equilibrium between the carbonate and the solution) and under water

78   (i.e., preventing fast release of CO_2 during carbonate precipitation) can potentially represent

79   carbonate deposits that would provide reliable clumped isotope temperatures as

80   demonstrated for the Devils Hole and Laghetto Basso calcites by Daëron et al. (2019).

81   Additionally, travertines that although precipitated from strongly degassing solutions, but

82   under water cover seem to form in clumped isotope equilibrium (Kele et al., 2015), in

83   contrast with stalagmite carbonate, which is precipitating from a thin solution film that

84   rapidly releases CO_2.

85   In this study we collected speleothem carbonates that were formed in cave-hosted

86   lakes, and gathered flowstone and travertine (both formed from flowing water) samples,

87   determined their clumped isotope compositions, and compared the Δ_{47}–based temperatures

88   with temperature data yielded by stable isotope analyses of inclusion-hosted water. In order

89   to obtain reliable inclusion-based data, this study discusses the effects of incomplete

90   removal of absorptively bound water or extraction of sample water. Finally, the study shows

91   that subaqueous carbonates can provide reliable paleotemperature archives in cave settings.

92

93   **Cave locations and samples**

94   The Nagy-tufa flowstone deposit is formed in the Béke Cave, Northern Hungary (N 48° 27'

95   39", E 20° 32' 34"). A detailed description of the cave site and the flowstone formation is

96   given in Demény et al. (2016). A core (BNT-2) was drilled from the flowstone and the BNT-2

97   top sample was gathered from the youngermost surface. The cave temperature was 10.0 °C

98   in the period of 2013-2015, preceding the collection date, hence this sample represents the

99   low-temperature cave environment among the studied materials.

100   Thermal karst environments are represented by the Berger Cave in Western Hungary

101   and the Molnár János Cave in Budapest, Central Hungary. The Molnár János Cave (N 47° 31'

102   05", E 19° 02' 09") contains a large underground lake, whose temperature is 23 ±1 °C, its pH

103   value is about 7.0, the $\delta^{18}O$ value is –10.8 ‰ (Virág, 2018). Calcite rafts were collected from

104   the Szt. Lukács shaft that were formed on the water surface and deposited on the bottom. A

105   special carbonate formation, morphologically resembling a volcano (hence called

106   „Vulkánok", „volcanos", Virág, 2018) were also collected. The cca. 20 cm large, cone-shaped

107   carbonate deposits (Fig. 1) have central chimneys, representing orifices of thermal water

108   emanations into an underground lake. The carbonate cones are made of coarse grained

109   calcite with abundant fluid inclusions (Fig. 1). The fluid inclusions are arranged in growth

110   zones within isometric calcite crystals, and hence can be regarded as primary. A travertine

111   calcite deposit was collected at the orifice of Szent Lukács well IV. The water temperature is

112   51.0 °C, the pH value is about 7.0, the $\delta^{18}O$ value is -11.7 ‰ (Virág, 2018).

113   The Berger Károly Cave is situated in an urban environment, under the settlement of

114   Tapolca (N 46° 53' 14", E 17° 26' 30"). The cave is strictly protected, only experts can enter

115   with the permission of the Balaton-felvidéki (the area north of Lake Balaton) National Park.

116   The cave was discovered releatively recently in 2022, the total length of shafts reaches about

117   2 km. The cave is a thermal karstic cave with abundant carbonate deposit decorations on the

118   walls, and several lakes, with thick calcite deposits (Fig. 1). The calcite deposits and local

119   physico-chemical parameters (water temperature, pH, chemical compositions) of two lakes

120   (Lángos and Titkok tava lakes) were investigated from 2020 to 2022, but only on 6 occasions

121   due to the restricted access of the lake chambers. The lakes are situated about 500 m away

122   from the artificial entrance. The Lángos Lake's and The Titkok tava lake's water temperatures

123   were 24.3 ±0.1 and 19.1 ±0.1 °C, respectively, in 2022 February and July, both lakes had pH

124   values of 7.4 ±0.1. 5x5 cm glass plates were placed just above and below the water levels

125   (Fig. 1) in February 2022 that were collected in July 2022. Visible carbonate deposition was

126   observed on the glass plates placed in the Lángos lake, from which plate #17 yielded enough

127   carbonate to study. Drill cores were collected from the lake carbonate deposits at two

128   locations in the Titkok tava and the Lángos lakes. Both cores were analysed at two sampling

129   points (Fig. 2A), as well as at the top where a carbonate crust was detected (L-top and T-top

130   for the Lángos and the Titkok tava, respectively) (Fig. 2). Fluid inclusions are usually primary,

131   scattered within isometric calcite crystals, are distributed in growth zones (Fig. 2B). The

132   carbonate crusts formed at the top of the drill cores are about 1 mm thick (Fig 2C). The

133   Lángos core's top crust contains needle-like crystals at its base, covered by isometric crystals

134   (Fig. 2D).

135

136   **Methods**

137   Petrographic analysis was conducted using a Nikon Eclipse E600 POL optical microscope on

138   polished thin (~100 µm) sections. The determination of mineral compositions of carbonate

139   crusts was carried out using a Rigaku D/Max Rapid II diffractometer, which was operated

140   with CuKα radiation at 50 kV and 0.6 mA. In situ analyses on a polished thin section surface

141   were conducted using a 100 µm collimator. A built-in CCD camera was used to select the

142   measurement areas. The IP was read by a laser scanning readout system in approximately 1

143   min. Acquisition time for each measurement was set to 5 minutes. 2DP RIGAKU software

144   was used to record the diffraction image from the laser readout, allowing the operator to

145   determine the area to integrate for a 2Θ versus intensity plot. This plot was read into the

146   RIGAKU PDXL 1.8 software for data interpretation.

147   Clumped stable isotope analyses of carbonates were carried out at the Isotope

148   Climatology and Environmental Research Centre (ICER), Institute for Nuclear Research

149   (ATOMKI), Debrecen. The analysis of carbonate samples was performed on a Thermo

150   Scientific^{TM} 253 Plus 10 kV Isotope Ratio Mass Spectrometer (IRMS), after phosphoric acid

151   digestion at 70 °C using a Thermo Scientific Kiel IV automatic carbonate device. 100–120 μg

152   aliquots of each carbonate sample measurement was replicated at least 8-12 times and

153   measured alongside carbonate standard samples. ETH1, ETH2, and ETH3 were used as

154   normalization standards, and IAEA-C2 was used as monitoring sample to determine the long-

155   term reproducibility of the instrument. Simultaneously with the clumped isotope analysis,

156   conventional carbonate stable isotope composition was also determined on the same

157   samples. Negative background, which is caused by secondary electrons on higher faraday-

158   cup detectors, was corrected by application of the pressure-sensitive baseline (PBL)

159   correction (Bernasconi et al. 2013) on all the raw beam signals. Peak scans at 5 different

160   intensities were used for PBL correction algorithm which is implemented in Easotope

161   Software (Release 20190125, concept by Cédric John, programmed by Devon Bowen) (John

162   and Bowen, 2016). The corrected data was exported into a csv file for further data

163   processing. Data evaluation, standardization, and analytical error propagation of Δ_{47}

164   clumped-isotope measurements was carried out with D47crunch python software (Daëron,

165   2021) using the revised IUPAC parameters for ^{17}O correction (Baertschi, 1976; Gonfiantini et

166   al., 1995; Meijer and Li, 1998; Assonov and Brenninkmeijer, 2003; Brand et al., 2010;

167   Bernasconi et al., 2018, Daëron et al., 2016; Schauer et al., 2016). Δ_{47} results are given in the

168   I-CDES90 scale (Bernasconi, et al. 2021), and apparent temperatures in °C were calculated

169   based on the Δ_{47}-temperature calibration from Anderson et al. (2021), with temperature

170   uncertainties propagated from the 1σ standard error (SE) of the Δ_{47} value.

171   Stable hydrogen and oxygen isotope compositions of inclusion-hosted water were

172   determined following the procedure of Demény et al. (2016). Sample chips (2-5 mm pieces)

173   of about 1-2 g were crushed under vacuum in 10 mm outer diameter stainless steel tubes,

174   the extracted H_2O was purified by vacuum distillation and the H_2O was introduced into a

175   liquid water isotope analyzer model LWIA-24d (Los Gatos Research Ltd.). The H_2O amount

176   was calibrated by injecting known water amounts. Corrections for measurement drifts,

177   amount effects and memory effects were conducted using three laboratory water standards

178   as described by Czuppon et al. (2014). The isotope compositions are expressed as δ^2H and

179      $\delta^{18}O$ values in ‰, relative to V-SMOW. The estimated analytical accuracies are about ±05

180   and ±2 ‰ for $\delta^{18}O_{fi}$ (where „fi" means „fluid inclusion") and δ^2H values, respectively (see

181   Demény et al., 2021). The present study investigated the effects of sample pre-heating and

182   extraction heating in details. In the laboratory of the IGGR the speleothem samples are

183   heated to 80 °C in order to remove absorptively bound water (Demény et al., 2016). In the

184   present study chips of a ~ 50 cm thick hydrothermal calcite vein (VK7) collected from a

185   Triassic limestone quarry (Tatabánya, W. Hungary; see Fig. 3 for optical microscopic fabrics)

186   were measured with various pre-heating conditions before crushing: (1) 80 °C under vacuum

187   for 2 hours; (2) 2 hours at 50 °C in an oven, 5 min vacuum pumping, flush with He at 80 °C for

188   15 min; and (3) flush with He at 80 °C for 15 min. In all cases H_2O extraction was done by

189   heating the sample to 120 °C for 5 min with continuous trapping at liquid nitrogen

190   temperature (Demény et al., 2016). Some extraction lines are kept in an oven with the same

191   pre-heating and extraction temperatures, hence the effect of low-temperature extraction at

192   80 °C was also investigated, and experiments (1) and (2) were repeated with 80 °C extraction

193   temperature (experiments 1' and 2', respectively).

194

195   **Results and Discussions**

196   *Effects of incomplete H_2O removal or extraction*

197   As Verheyden et al. (2008) detected, some speleothem samples show inclusion

198   decrepitation at 100 °C (which otherwise would be needed to achieve 100% sorption water

199   removal). The effect is especially strong when the speleothem sample abundantly contains

200   large inclusions (e.g., sample CSB of Fig. 3) that cannot survive heating above 80 °C. Apart

201   from the H_2O content decrease, the remaining H_2O may be fractionated by the preferential

202   removal of light isotopes, resulting in an evaporation-like δ^2H-$\delta^{18}O$ distribution. In order to

203   avoid partial decrepitation, Demény et al. (2016) decided to use pre-heating at 80 °C.

204   However, most laboratories dealing with inclusion-hosted water isotope analyses apply >100

205   °C pre-heating (115-120 °C: Dublyansky and Spötl, 2009; Arienzo et al., 2013; Dassié et al.,

206   2018; de Graaf et al., 2020; Warken et al., 2022; Weissbach et al., 2023; 130 °C: Vonhof et

207   al., 2006; 140 °C: Affolter et al., 2014; 2019) in a He (e.g., Vonhof et al., 2006; Dublyansky

208   and Spötl, 2009) or in N_2 flow (e.g., Arienzo et al., 2013). The removal of sorption water is

209   monitored by recording water signals in a mass spectrometer or in a laser spectroscope.

210   Czuppon et al. (2014) and Demeny et al. (2016) used a different approach, the samples were

211   heated only to 80 °C, but pumped to a high vacuum for 2 hours reaching a constant vacuum

212   of 10^{-3} mbar. The analytical accuracy was tested by analysing speleothems with known

213   isotopic compositions (Demény et al., 2021), suggesting that the long vacuum pumping

214   technique is effective enough to remove sorption water. The inevitable drawback is the

215   analytical throughput, which is certainly higher for the short-time 120 °C flushing method.

216   However, if other systems are changed to this low-temperature heating with short-time

217   inert gas flushing in order to avoid decrepitation, the effect of incomplete H_2O removal has

218   to be determined. On the other hand, some extraction lines are placed in ovens (e.g.,

219   Affolter et al., 2014; Weissbach et al., 2023), whose temperature is not easily adjusted to

220   higher temperatures required for the sample H_2O extraction. Hence, the effect of

221   incomplete H_2O extraction was also investigated.

222   The results of pre-heating and extraction temperature experiments are shown in Fig.

223   4. Firth the pre-heating effect is discussed when after-crushing extraction was conducted at

224   120 °C. The experiment with 80 °C pre-heating under vacuum (experiment 1) yielded $\delta^2H=-$

225   61.8 ±1.8 ‰ and $\delta^{18}O_{fi}=-7.6$ ±0.1 ‰ (n=4). The experiment with 2 hours in a 50 °C oven,

226   followed by 5 min vacuum pumping and He flush for 15 min at 80 °C (experiment 2) resulted

227   in a large scatter, some results matching the data of experiment 1, some others shifted in

228   negative $\delta^{18}O$ direction. Experiment 3 was conducted only with 15 min He flushing before

229   crushing and yielded δ^2H and $\delta^{18}O_{fi}$ values negatively shifted (−63.3 ±3.0 and −8.7 ±0.4 ‰,

230   respectively) with increased scatter. These observations indicate that the 15 min 80 °C He

231   flushing did not remove the absorptively bound water that originated from the local

232   moisture, and the 2 hours vacuum pumping or longer He flushing is needed at 80 °C.

233   The effect of low extraction temperature was investigated by repeating experiments

234   1 and 2 but with heating to 80 °C after crushing and during H_2O collection. The rationale is

235   that if the extraction line is held in an oven with constant temperature and pre-heating is

236   conducted at 80 °C, then extraction may also be done at this temperature. Experiment 1' (2

237 hours pumping and extraction at 80 °C) yielded altered δ^2H (–62.2 ±7.7 ‰) and $\delta^{18}O_{fi}$ (–9.8

238 ±0.3 ‰), strongly shifted from the results of experiment 1 (Fig. 4). Experiment 2' (50 °C oven,

239 5 min vacuum, 15 min He flush, and extraction at 80 °C) yielded δ^2H and $\delta^{18}O_{fi}$ values close

240 to the shifted ones of experiment 2. These data indicate that a part of the sample water

241 remained on the freshly crushed calcite surface, and molecules enriched in light isotopes are

242 preferentially extracted. As a conclusion, it is suggested that either the samples are pumped

243 or flushed for a longer time at 80 °C, but the extraction has to be done at >120 °C, or the

244 samples' behavior during >100 °C flushing has to be carefully monitored in order to detect

245 sensitive samples, whose heating may alter the isotopic compositions. Inclusion

246 petrographic studies prior to isotope analyses are also suggested to detect samples with

247 large, and hence decrepiation-sensitive inclusions. However, the present study and the

248 earlier comparisons of samples with known isotopic compositions show that the 80 °C

249 vacuum pumping method can effectively remove sorption water and yield reliable results.

250

251 *Clumped isotope temperatures vs. measured or inclusion-based temperatures*

252 The most straightforward test of clumped isotope based temperature determinations is the

253 comparison with measured formation temperatures of recently formed calcites (e.g., Kele et

254 al., 2015). The results of the present study are listed in Supplementary Table 1. The Nagy-

255 tufa flowstone deposit (sample BNT-2 top) of the Béke Cave yielded a Δ_{47} value of 0.6383

256 ±0.0094 ‰ (I-CDES90°C, Crunch, ±1SE, as all Δ_{47} data in the followings) that corresponds to a

257 formation temperature of 10.3 ±2.7 °C using the Anderson et al. (2021) calibration (applied

258 for all Δ_{47} temperatures in the followings), as compared with the measured cave

259 temperature of 9.8 °C (Czuppon et al., 2018). The calcite rafts formed at 23.2 °C on the lake

260   surface of the Molnár János Cave (sample M3) yielded Δ_{47}=0.5855 ±0.0088, corresponding to

261   27.1 ±3.1 °C. The third occurrence was a travertine deposit formed at the orifice of the

262   Lukács IV thermal well at 51.0 °C (sample M2) that yielded a Δ_{47} value of 0.5295 ±0.0083 ‰,

263   corresponding to 48.7 ±3.5 °C. These data are plotted in Fig. 5 that shows the clumped

264   isotope based temperatures as a function of measured or inclusion-based temperatures. The

265   three samples with measured formation temperatures define a linear correlation that fit the

266   1:1 line within the analytical precision. Hence the applied clumped isotope technique and

267   the sample selection approach are appropriate for further evaluation.

268   The drill core samples collected in the Berger Károly Cave were studied in details as

269   the glass plates placed under water and the uppermost surfaces of drill cores are covered by

270   actively forming carbonate crust (Fig. 2C), hence their compositions can be directly

271   compared with monitoring data, and as the drill core calcites contain abundant primary fluid

272   inclusions (Fig. 2B), whose water content could be analysed for stable H and O isotope

273   compositions. Glass plates placed under water on the carbonate deposit in both lakes

274   seldom contained enough carbonate to analyse, but plate #17 provided enough calcite

275   (tested by XRD measurement). The plate #17 calcite yielded a Δ_{47} value of 0.6046 ±0.0145 ‰

276   (20.7 ±4.7 °C), close to the measured water temperature (24.3 °C). The carbonate crust of

277   the Titkok Tava (sample T-top) is made of 100% calcite, whereas the carbonate collected

278   from the Lángos drill core's top (sample L-top) for clumped isotope analysis contained

279   aragonite detected by powder XRD analysis. As Figs. 2C and D show, the carbonate crust

280   starts with a layer of needle-like crystals, and then it is covered by isometric crystals. Micro-

281   XRD analyses proved, that the needle-like crystal layer is aragonite, and the covering

282   carbonate is calcite. The L-top sample collected for clumped isotope analysis was a mixture

283   of the two carbonates (approximately 35% calcite and 65% aragonite). However, the Δ_{47}

284   temperature (19.5 ±3.3 °C) is close to the measured water temperature of the lake (24.3 °C),

285   indicating that the presence of aragonite does not affect the clumped isotope temperature

286   determination. This is in agreement with the results of de Winter et al. (2022), who found

287   that aragonite and calcite behave similarly in terms of clumped isotope geochemistry. The

288   carbonate crust of the Titkok Tava drill core (T-top) is made of calcite and its Δ_{47} temperature

289   (23.8 ±3.4 °C) is also close to the measured water temperatures (19.1 °C). These data are

290   plotted in Fig. 5, fitting the 1:1 line within the analytical uncertainties.

291   Apart from the measured water temperatures, the Δ_{47} temperatures can be

292   compared with inclusion-based data. The Lángos and Titkok drill cores were sampled at two

293   points (samples L1, L2, T1, T2), the δ^2H and $\delta^{18}O$ values were determined in duplicates

294   (Supplementary Table 1). Formation temperatures were calculated using average $\delta^{18}O_{fi}$

295   values, $\delta^{18}O_{cc}$ data, and the calcite-water oxygen isotope fractionation equation of Johnston

296   et al. (2013). The reason of selecting the Johnston et al. (2013) equation was that the $\delta^{18}O$

297   value of the L-top calcite and the lake water yielded 22.9 ±0.5 °C using the Johnston

298   equation close to the measured lake water temperature (24.3 °C), whereas other equations

299   yielded lower (20.0 °C, Friedman and O'Neil, 1977) or higher (26.6 °C, Daëron et al., 2019)

300   temperatures. The average Δ_{47} temperatures of the L1-L2 and T1-T2 samples are 24.7 ±2.0 °C

301   and 20.4 ±4.1 ℃, respectively, which values are equal to the present day water

302   temperatures (24.3 and 19.1 °C, respectively) within the analytical uncertainties. The data

303   were plotted also in Fig. 5 as a function of inclusion-based temperatures. The good

304   agreements of Δ_{47} and measured water temperatures, and the good fit to the 1:1 line in Fig 5

305   indicate both a long-term temperature stability in the cave and that the subaqueous calcites

306   work well for both the clumped isotope and the inclusion isotope studies.

307   The „Vulkánok" sample provides a fossil example of subaqueous carbonates. The

308   inclusion-hosted water was analysed along with the Δ_{47} measurements and the calculated

309   temperatures are plotted in Fig. 5. The inclusion-based temperature (42 ±5 °C) is slightly

310   lower than the Δ_{47} temperature (53 ±4 °C). One possibility is that the formation temperature

311   and the present day ambient temperature (about 20 °C in the Molnár János Cave) is so

312   different that the host calcite and the inclusion water have undergone post-formation

313   oxygen isotope exchange, leading to negative $\delta^{18}O_{fi}$ shift due to the mass difference

314   between the calcite and the water. This explanation is supported by the observation that the

315   hydrogen isotope compositions of the nearby thermal well (Lukács IV, −85.0 ‰) and the

316   Vulkánok inclusion water (−86.2 ‰) are very close to each other, whereas the $\delta^{18}O$ values (−

317   11.7 and −13.7 ‰, respectively) are significantly different. These data indicate that the

318   Vulkánok carbonate cones were deposited from a thermal water similar to that of the Lukács

319   IV well. Using the −11.7 ‰ $\delta^{18}O_{water}$ value, the Johnston et al (2013) equation yields 54 ±5 °C,

320   which is very close to that of the Lukács IV well temperature (51.1 °C) and to the Δ_{47}

321   temperature (53 ±4 °C). The effect of re-equilibration is marked by an arrow in Fig.5, shifting

322   the temperature from the 1:1 line to a lower inclusion-based value. Hence the inclusion

323   $\delta^{18}O_{fi}$ -based paleotemperature calculation is only a rough estimation at or above 40-50 °C,

324   whereas the clumped isotope measurements can yield reliable temperatures for subaqueous

325   carbonates.

326   **Conclusions**

327   Cave-hosted subaqueous carbonate deposits were investigated by means of clumped

328   isotope analyses and measurements of stable isotope compositions of inclusion-hosted

329   waters in order to determine if they yield reliable paleotemperature data. First the analytical

330 method of inclusion water analysis was investigated to determine the effect of sample

331 preheating. For the analytical setup used in this study (vacuum crushing in a line attached to

332 a laser spectroscope), the most reliable data were produced by heating the samples to 80 °C

333 for 2 hours to reach an end vacuum of $<10^{-3}$ mbar. Helium flushing for 15 min at 80 °C may

334 not remove the absorptively bound water. H_2O extraction is incomplete at 80 °C, for the

335 collection of sample H_2O heating to 120 °C is needed.

336 Clumped isotope analyses of carbonate deposits with known formation temperatures

337 (flowstone, travertine, calcite rafts, lake deposits) yielded close-to-measured temperatures,

338 priving that such deposits provide reliable temperature data. Subaqueous carbonate

339 deposits formed in cave-hosted lakes were investigated also by stable isotope analyses of

340 inclusion-hosted waters that – together with the stable oxygen isotope composition of the

341 host carbonate – yielded realistic formation temperatures. These data indicate that

342 subaqueous carbonate speleothems are valuable paleotemperature archives as kinetic

343 isotope fractionations do not affect them significantly in the underwater environment.

References

Affolter, S., Fleitmann, D., Leuenberger, M., 2014. New online method for water isotope analysis of speleothem fluid inclusions using laser absorption spectroscopy (WS-CRDS). *Climate of the Past* 10, 1291-1304. https://doi.org/10.5194/cp-10-1291-2014

Affolter, S. , Häuselmann, A., Fleitmann, D., Edwards, R. L., Cheng, H., Leuenberger, M., 2019. Central Europe temperature constrained by speleothem fluid inclusion water isotopes over the past 14,000 years. *Science Advances* 5, eaav3809. DOI: 10.1126/sciadv.aav3809

Anderson, N.T., Kelson, J.R., Kele, S., Daëron, M., Bonifacie, M., Horita, J., Mackey, T.J., John, C.M., Kluge, T., Petschnig, P., Jost, A.B., Huntington, K.W., Bernasconi, S.M., Bergmann, K.D., 2021. A Unified Clumped Isotope Thermometer Calibration (0.5–1,100°C) Using Carbonate-Based Standardization. Geophysical Research Letters 48, 1-11. https://doi.org/10.1029/2020GL092069

Arienzo, M. M., Swart, P.K., Vonhof, H.B., 2013. Measurement of $\delta^{18}O$ and $\delta^{2}H$ values of fluid inclusion water in speleothems using cavity ring-down spectroscopy compared with isotope ratio mass spectrometry. *Rapid Communications in Mass Spectrometry* 27, 2616-2624. https://doi.org/10.1002/rcm.6723

Assonov, S.S., Brenninkmeijer, C.A.M., 2003. A redetermination of absolute values for 17_{RVPDB}-CO_2 and 17_{RVSMOW}. *Rapid Communications in Mass Spectrometry* 17, 1017-1029. DOI: 10.1002/rcm.1011

Baertschi, P., 1976. Absolute ^{18}O content of standard mean ocean water. Earth and Planetary Science Letters 31, 341-344. https://doi.org/10.1016/0012-821X(76)90115-1

Bernasconi, S. M., Hu, B., Wacker, U., Fiebig, J., Breitenbach, S. F. M., Rutz, T., 2013. Background effects on Faraday collectors in gas source mass spectrometry and implications for clumped isotope measurements. *Rapid Communications in Mass Spectrometry* 27, 603-612. https://doi.org/10.1002/rcm.6490

Bernasconi, S.M., Müller, I.A., Bergmann, K.D., Breitenbach, S.F.M., Fernandez, A., Hodell, D.A., Jaggi, M., Meckler, A.N., Millan, I., Ziegler, M., 2018. Reducing uncertainties in carbonate clumped isotope analysis through consistent carbonate-based standardization. *Geochemistry, Geophysics, Geosystems* 19, 2895-2914. https://doi.org/10.1029/2017GC007385

384   Bernasconi, S.M., Daëron, M., Bergmann, K.D., Bonifacie, M., Meckler, A.N., Affek, H.P., et

385   al., 2021. InterCarb: A community effort to improve interlaboratory standardization

386   of the carbonate clumped isotope thermometer using carbonate standards.

387   *Geochemistry, Geophysics, Geosystems* 22, e2020GC009588.

388   https://doi.org/10.1029/2020GC00958810.1029/2020GC009588

389   Brand, W.A., Assonov, S.S., Coplen, T.B., 2010. Correction for the ^{17}O interference in δ(13C)

390   measurements when analyzing CO_2 with stable isotope mass spectrometry (IUPAC

391   Technical Report). *Pure and Appled Chemistry* 82, 1719–1733.

392   https://doi.org/10.1351/PAC-REP-09-01-05

393   Coplen, T.B., 2007. Calibration of the calcite-water oxygen-isotope geothermometer at

394   Devils Hole, Nevada, a natural laboratory. *Geochimica et Cosmochimica Acta* 71,

395   3948-3957. https://doi.org/10.1016/j.gca.2007.05.028

396   Czuppon, Gy., Ramsay, R.R., Özgenc, I., Demén,y A., Gwalani, L.G., Rogers, K., Eves, A., Papp,

397   L., Palcsu, L., Berkesi, M., Downes, P.J., 2014. Stable (H, O, C) and noble-gas (He and

398   Ar) isotopic compositions from calcite and fluorite in the Speewah Dome, Kimberley

399   Region, Western Australia: implications for the conditions of crystallization and

400   evidence for the influence of crustal-mantle fluid mixing. *Mineralogy and Petrology*

401   108, 759-775. https://doi.org/10.1007/s00710-014-0333-7

402   de Graaf, S., Vonhof, H.B., Weissbach, T., Wassenburg, J.A., Levy, E.J., Kluge, T., Haug, G.H.,

403   2020. A comparison of isotope ratio mass spectrometry and cavity ring-down

404   spectroscopy techniques for isotope analysis of fluid inclusion water. *Rapid*

405   *Communications in Mass Spectrometry* 34, e8837. DOI: 10.1002/rcm.8837

406   de Winter, N. J., Witbaard, R., Kocken, I. J., Müller, I. A., Guo, J., Goudsmit, B., Ziegler, M.,

407   2022. Temperature dependence of clumped isotopes ($Δ_{47}$) in aragonite. *Geophysical*

408   *Research Letters* 49, e2022GL099479. https://doi.org/10.1029/2022GL099479

409   Daëron, M., Blamart, D., Peral, M., Affek, H.P., 2016. Absolute isotopic abundance ratios and

410   the accuracy of $Δ_{47}$ measurements. *Chemical Geology* 442, 83-96.

411   https://doi.org/10.1016/j.chemgeo.2016.08.014

412   Daëron, M., Drysdale, R. N., Peral, M., Huyghe, D., Blamart, D., Coplen, T. B., Lartaud, F. ,

413   Zanchetta, G., 2019. Most Earth-surface calcites precipitate out of isotopic

414   equilibrium. Nature Communications 10, 429. https://doi.org/10.1038/s41467-019-

415   08336-5

416   Daëron, M., 2021. Full Propagation of Analytical Uncertainties in Δ_{47} Measurements,

417   Geochemistry, Geophysics, Geosystems 22, E2020GC009592.

418   https://doi.org/10.1029/2020GC009592

419   Dassié, E. P., Genty, D., Noret, A., Mangenot, X., Massault, M., Lebas, N., Duhamel, M.,

420   Bonifacie, M., Gasparrini, M., Minster, B., Michelot, J.-R., 2018. A newly designed

421   analytical line to examine fluid inclusion isotopic compositions in a variety of

422   carbonate samples. Geochemistry, Geophysics, Geosystems 19.

423   https://doi.org/10.1002/2017GC007289

424   Deininger, M., Hansen, M., Fohlmeister, J., Schröder-Ritzrau, A., Burstyn, Y., Scholz, D., 2021.

425   Are oxygen isotope fractionation factors between calcite and water derived from

426   speleothems systematically biased due to prior calcite precipitation (PCP)?

427   *Geochimica et Cosmochimica Acta* 305, 212-227.

428   https://doi.org/10.1016/j.gca.2021.03.026

429   Demény, A., Kele, S., Siklósy, Z., 2010. Empirical equations for the temperature dependence

430   of calcite-water oxygen isotope fractionation from 10 to 70 °C. *Rapid*

431   *Communications in Mass Spectrometry* 24, 3521-3526.

432   https://doi.org/10.1002/rcm.4799

433   Demény, A., Czuppon, Gy., Kern, Z., Leél-Őssy, Sz., Németh, A., Szabó, M., Tóth, M., Wu, Ch-

434   Ch., Shen,Ch.-Ch., Molnár, M., Németh, T., Németh, P., Óvári, M., 2016.

435   Recrystallization-induced oxygen isotope changes in inclusion-hosted water of

436   speleothems – Paleoclimatological implications. *Quaternary International* 415, 25-32.

437   https://doi.org/10.1016/j.quaint.2015.11.137

438   Demény, A., Rinyu, L., Kern, Z., Hatvani, I.G., Czuppon, Gy., Surányi, G., Leél-Őssy, Sz., Shen.,

439   Ch.-Ch., Koltai, G., 2021. Paleotemperature reconstructions using speleothem fluid

440   inclusion analyses from Hungary. *Chemical Geology* 563, 120051.

441   https://doi.org/10.1016/j.chemgeo.2020.120051

442   Duan, W., Wang, X., Tan, M., Cui, L., Wang, X., Xiao, Z., 2022. Variable phase relationship

443   between monsoon and temperature in East Asia during Termination II revealed by

444   oxygen and clumped isotopes of a northern Chinese stalagmite. *Geophysical Research*

445   *Letters* 49, e2022GL098296. https://doi.org/10.1029/2022GL098296

446   Dublyansky, Y. V., Spötl, C., 2009. Hydrogen and oxygen isotopes of water from inclusions in

447   minerals: design of a new crushing system and on-line continuous-flow isotope ratio

448   mass spectrometric analysis. *Rapid Communications in Mass Spectrometry* 23, 2605-

449   2613. DOI: 10.1002/rcm.4155

450   Eiler, J. M., 2007. "Clumped-isotope" geochemistry—The study of naturally-occurring,

451   multiply-substituted isotopologues. *Earth and Planetary Science Letters* 262, 309-327.

452   https://doi.org/10.1016/j.epsl.2007.08.020

453   Fairchild, I.J., Baker, A., 2012. Speleothem Science. – Wiley-Blackwell, 450 pp.

454   Friedman, I., O'Neil, J.R., 1977. Compilation of stable isotope fractionation factors of

455   geochemical interest. In: *Data of Geochemistry* (6th edition). U.S. Geological Survey,

456   Professional Paper 440-KK.

457   Ghosh, P., Adkins, J., Affek, H., Balta, B., Guo, W., Schauble, E.A., Schrag, D., Eiler, J.M., 2006.

458       $^{13}C–^{18}O$ bonds in carbonate minerals: a new kind of paleothermometer. *Geochimica*

459   *et Cosmochimica Acta* 70, 1439-1456. https://doi.org/10.1016/j.gca.2005.11.014

460   Gonfiantini, R., Stichler, W., Rozanski, K., 1995. Standards and intercomparison materials

461   distributed by the International Atomic Energy Agency for stable isotope

462   measurements. In Reference and Intercomparison Materials for Stable Isotopes of

463   Light Elements. International Atomic Energy Agency, Vienna. IAEA-TECDOC-825, pp.

464   13-29.

465   Jautzy, J.J., Savard, M.M., Dhillon, R.S., Bernasconi, S.M., Smirnoff, A., 2020. Clumped isotope

466   temperature calibration for calcite: Bridging theory and experimentation.

467   *Geochemical Perspectives Letters* 14, 36-41. doi: 10.7185/geochemlet.2021

468   John, C.M., Bowen, D., 2016. Community software for challenging isotope analysis: First

469   applications of 'Easotope' to clumped isotopes. *Rapid Communications in Mass*

470   *Spectrometry* 30, 2285-2300. https://doi.org/10.1002/rcm.7720

471   Johnston, V.E., Borsato, A., Spötl, C., Frisia, S., Miorandi, R., 2013. Stable isotopes in caves

472   over altitudinal gradients: fractionation behaviour and inferences for speleothem

473   sensitivity to climate change. *Climate of the Past* 9, 99-118.

474   https://doi.org/10.5194/cp-9-99-2013

475   Kele, S., Breitenbach, S. F. M., Capezzuoli, E., Meckler, N., Ziegler, M., Millan, I. M., Kluge, T.,

476   Deák, J., Hanselmann, K., John, C. M., Yan, H., Liu, Z., Bernasconi, S. M., 2015.

477   Temperature dependence of oxygen- and clumped isotope fractionation in

478   carbonates: A study of travertines and tufas in the 6–95 °C temperature range.

479   *Geochimica et Cosmochimica Acta* 168, 172-192.

480   https://doi.org/10.1016/j.gca.2015.06.032

481 Koehler, G.D., Chipley, D., Kyser, T.K., 1991. Measurement of the hydrogen and oxygen

482   isotopic compositions of concentrated chloride brines and brines from fluid inclusions

483   in halite. *Chemical Geology* 94, 45-54. https://doi.org/10.1016/S0009-

484   2541(10)80016-6

485 Lachniet, M. S. (2009): Climatic and environmental controls on speleothem oxygen-isotope

486   values. *Quaternary Science Reviews* 28, 412-432.

487   https://doi.org/10.1016/j.quascirev.2008.10.021

488 Meckler A.N., Affolter S., Dublyansky Y.V., Krüger Y., Vogel N., Bernasconi S.M., Frenz M.,

489   Kipfer R., Leuenberger M., Spötl C., Carolin S., CobbK.M., Moerman J., Adkins J.F.,

490   Fleitmann D., 2015. Glacial-interglacial temperature change in the tropical West

491   Pacific: A comparison of stalagmite-based paleo-thermometers. *Quaternary Science*

492   *Reviews* 127, 90-116. https://doi.org/10.1016/j.quascirev.2015.06.015

493 Meijer, H.A.J., Li, W.J., 1998. The use of electrolysis for accurate $\delta^{17}O$ and $\delta^{18}O$ isotope

494   measurements in water. Isotopes in Environmental and Health Studies 34, 349-369.

495   https://doi.org/10.1080/10256019808234072

496 O'Neil, J.R., Epstein, S., 1966. A method for oxygen isotope analysis of milligram quantities of

497   water and some of its applications. *Journal of Geophysical Research* 71, 4955-4961.

498   https://doi.org/10.1029/JZ071i020p04955

499 O'Neil, J.R., Clayton, R., Mayeda, T., 1969. Oxygen isotopic fractionation in divalent metal

500   carbonates. *The Journal of Chemical Physics* 51, 5547-5558.

501   https://doi.org/10.1063/1.1671982

502 Schauer, A.J., Kelson, J., Saenger, C., Huntington, K.W., 2016. Choice of ^{17}O correction affects

503   clumped isotope (Δ_{47}) values of CO_2 measured with mass spectrometry. *Rapid*

504   *Communications in Mass Spectrometry* 30, 2607-2616.

505   https://doi.org/10.1002/rcm.7743

506 Socki, R.A., Romanek, C.S., Gibson, Jr., E.K., 1999. On-Line technique for measuring stable

507   oxygen and hydrogen isotopes from microliter quantities of water. *Analytical*

508   *Chemistry* 71, 2250-2253. DOI: 10.1021/ac981140i

509 Tremaine, D. M., Froelich, P. N., Wang, Y., 2011. Speleothem calcite farmed in situ: Modern

510   calibration of $\delta^{18}O$ and $\delta^{13}C$ paleoclimate proxies in a continuously-monitored natural

511   cave system. *Geochimica et Cosmochimica Acta* 75, 4929-4950.

512   https://doi.org/10.1016/j.gca.2011.06.005

513 Verheyden, S., Genty, D., Cattani, O., van Breukelen, M. R., 2008. Water release patterns of

514   heated speleothem calcite and hydrogen isotope composition of fluid inclusions.

515   *Chemical Geology* 247, 266-281. https://doi.org/10.1016/j.chemgeo.2007.10.019

516 Virág, M., 2018. Hypogene and epigene karstic processes and their influence on the

517   evolution of the Rózsadomb caves in Buda – by the example of Szemlő-hegy and

518   Molnár János Cave. PhD Thesis, Eötvös Loránd University, pp. 172. DOI:

519   10.15476/ELTE.2018.156

520 Vonhof, H. B., van Breukelen, M. R., Postma, O., Rowe, P. J., Atkinson, T. C., Kroon, D., 2006.

521   A continuous-flow crushing device for on-line δ^2H analysis of fluid inclusion water in

522   speleothems. Rapid Communications in Mass Spectrometry 20, 2553-2558.

523   https://doi.org/10.1002/rcm.2618

524 Warken, S. F., Weißbach, T., Kluge, T., Vonhof, H., Scholz, D., Vieten, R., Schmidt, M., Winter,

525   A., Frank, N., 2022. Last glacial millennial-scale hydro-climate and temperature

526   changes in Puerto Rico constrained by speleothem fluid inclusion δ^{18}O and δ^2H

527   values. *Climate of the Past* 18, 167-181. https://doi.org/10.5194/cp-18-167-2022

528 Weissbach, T., Kluge, T., Affolter, S., Leuenberger, M.C., Vonhof, H., Riechelmann, D.F.C.,

529   Fohlmeister, J., Juhl, M.-C., Hemmer, B., Wu, Y., Warken, S.F., Schmidt, M., Frank, N.,

530   Aeschbach, W., 2023. Constraints for precise and accurate fluid inclusion stable

531   isotope analysis using water-vapour saturated CRDS techniques. *Chemical Geology*

532   617, 121268. https://doi.org/10.1016/j.chemgeo.2022.121268

533 Yonge, C. J., 1982. Stable Isotope Studies of Water Extracted from Speleothems. PhD thesis,

534   McMaster University, Hamilton, ON, Canada. pp. 270.

535

Figure captions

Fig. 1. A) The Vulkánok („volcanos") carbonate cones in the Molnár János Cave (photo by Dénes Szieberth). B) Optical microscopic picture with crossed nicols of the Vulkánok carbonate. C) The Lángos Lake of the Berger Károly Cave. Glass plates were placed on the calcite deposit at the upper left corner of the lake shore. D) Core drilling at the Titkok Tava lake in the Berger Károly Cave.

Fig. 2. Drill cores from the Titkok Tava lake (samples „T") and from the Lángos Lake (samples „L"). B) Optical microscopic picture (one nicol) from the middle of the Lángos drill core. C) The top of the Lángos drill core with thin carbonate crust. D) Optical microscopic picture (one nicol) of the carbonate crust of the Lángos drill core.

Fig. 3. Optical microscopic pictures (one nicol) of samples VK7 analysed in this study and sample CSB of Demény et al. (2016).

Fig. 4. Stable hydrogen and oxygen isotope compositions (δ^2H and $\delta^{18}O$ values, respectively, in ‰ relative to V-SMOW) of inclusion-hosted water of sample VK7 analysed using various pre-heating and extraction temperatures. GMWL: Global Meteoric Water Line.

Fig. 5. Formation temperatures obtained by clumped isotope analyses as a function of measured water temperatures or formation temperatures calculated from the oxygen isotope fractionations between carbonate and inclusion-hosted water.

Figure 1

0.1 mm

Figure 2

Figure 3

0.1 mm   Sample VK7

0.1 mm   Sample CSB
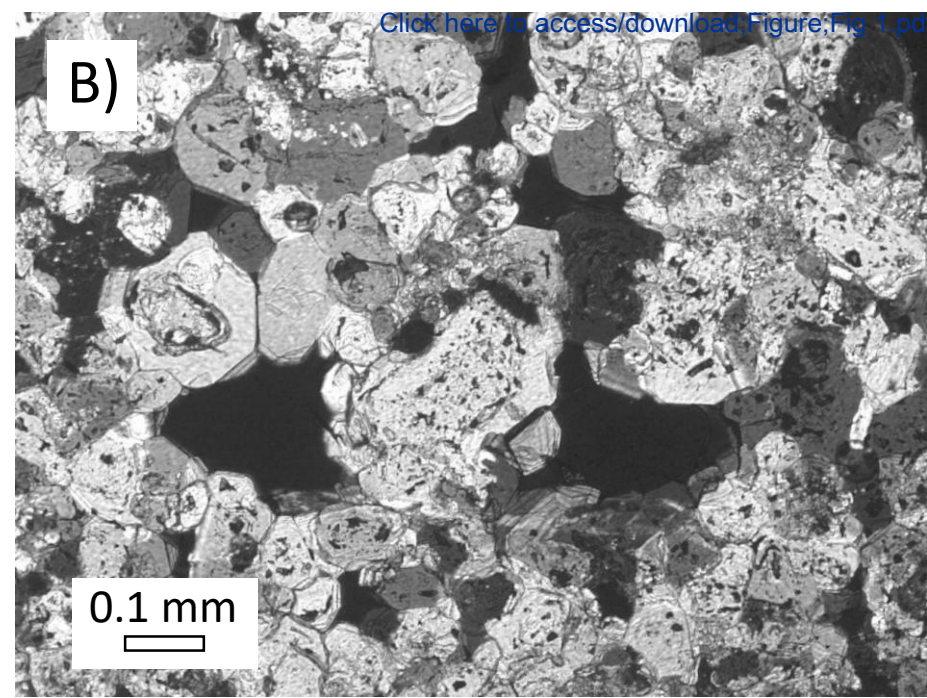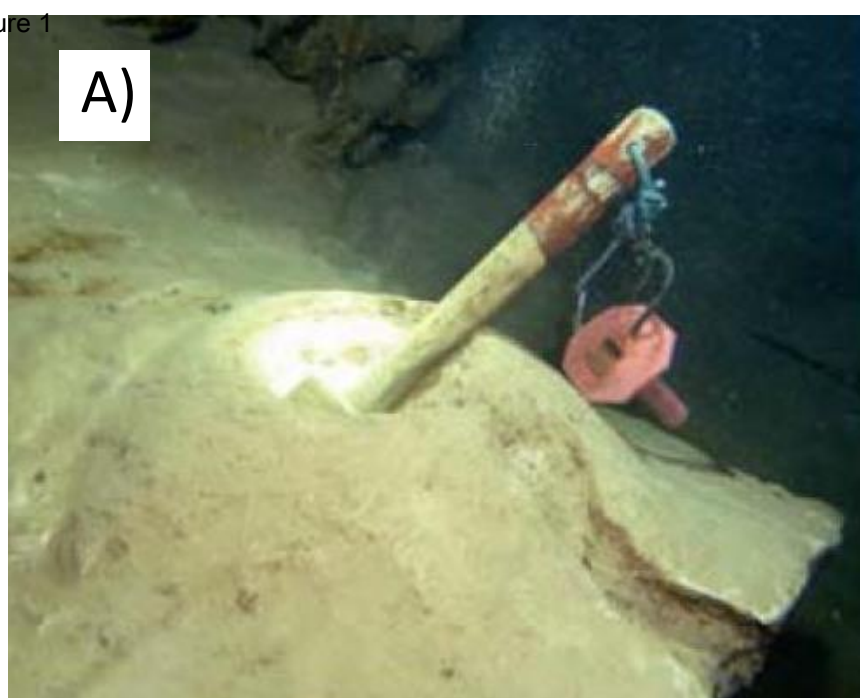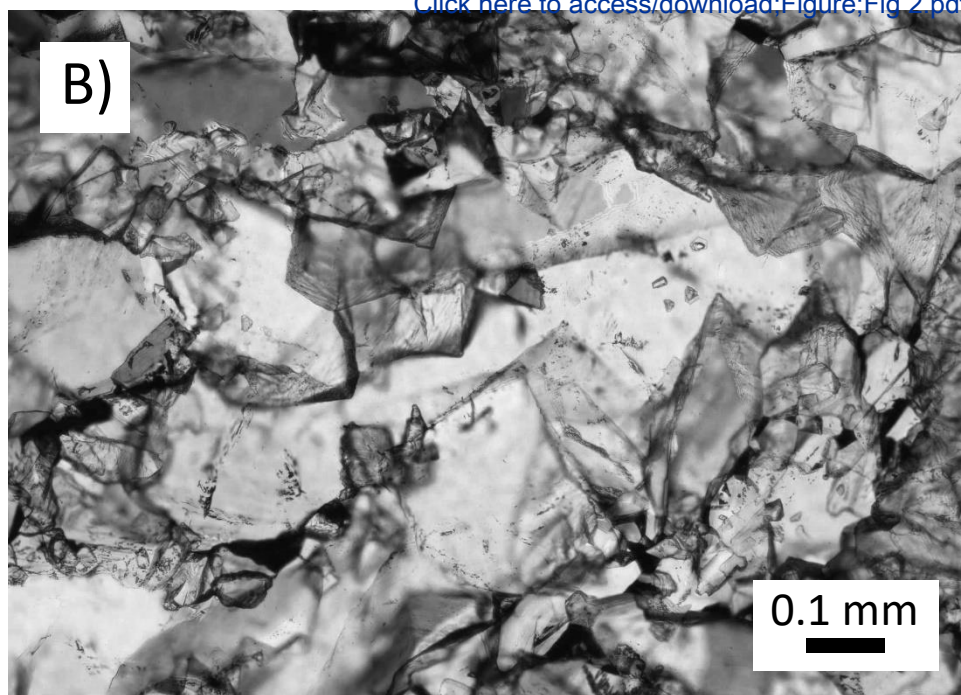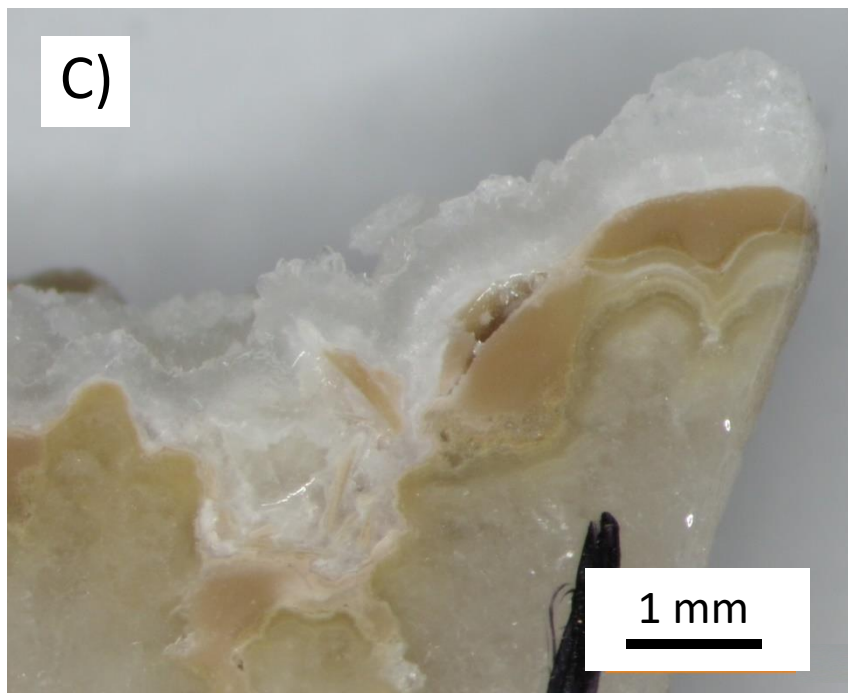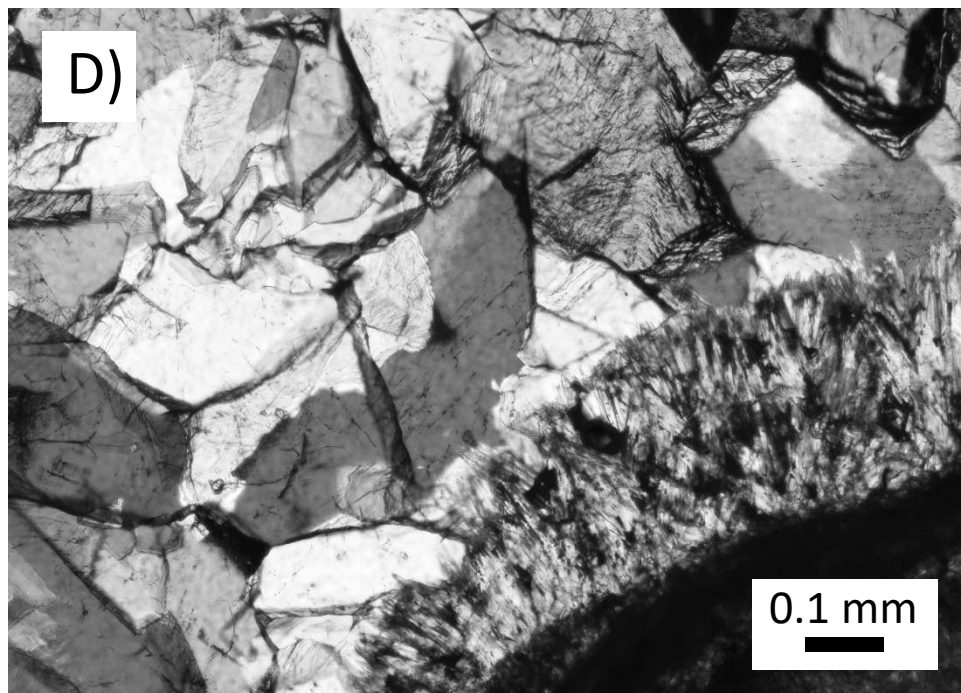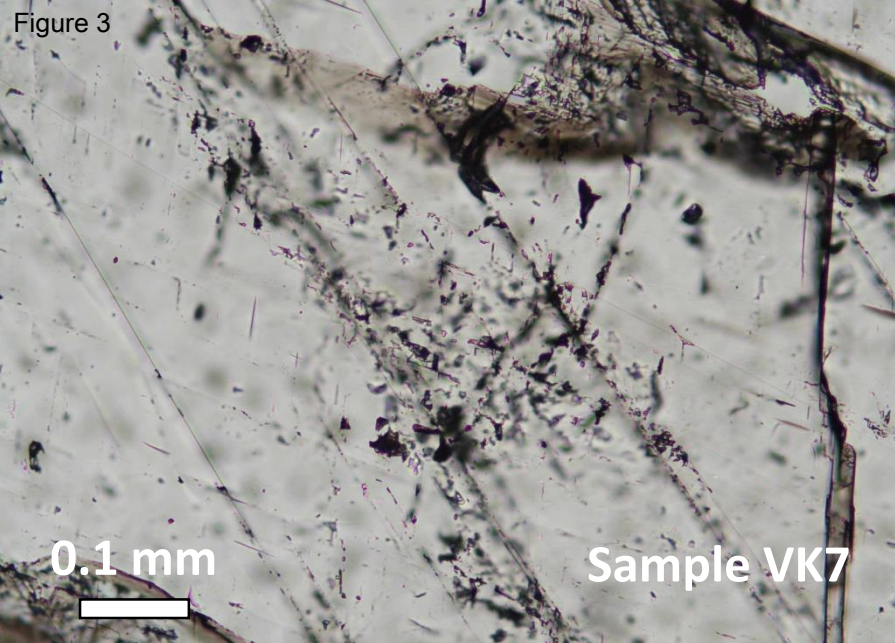
Figure 4

Figure 5

Click here to access/download;Figure;Fig 5.pdf ⬇
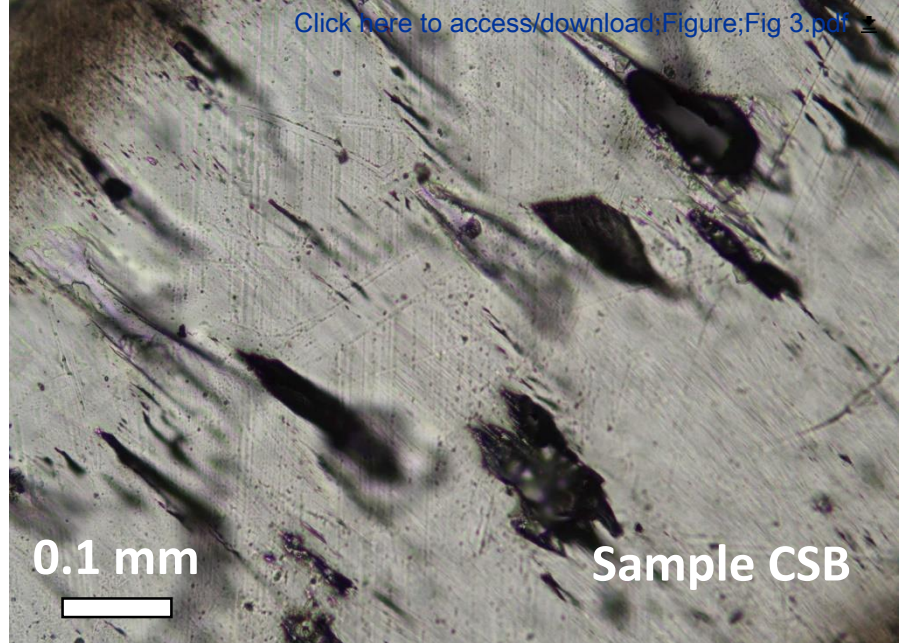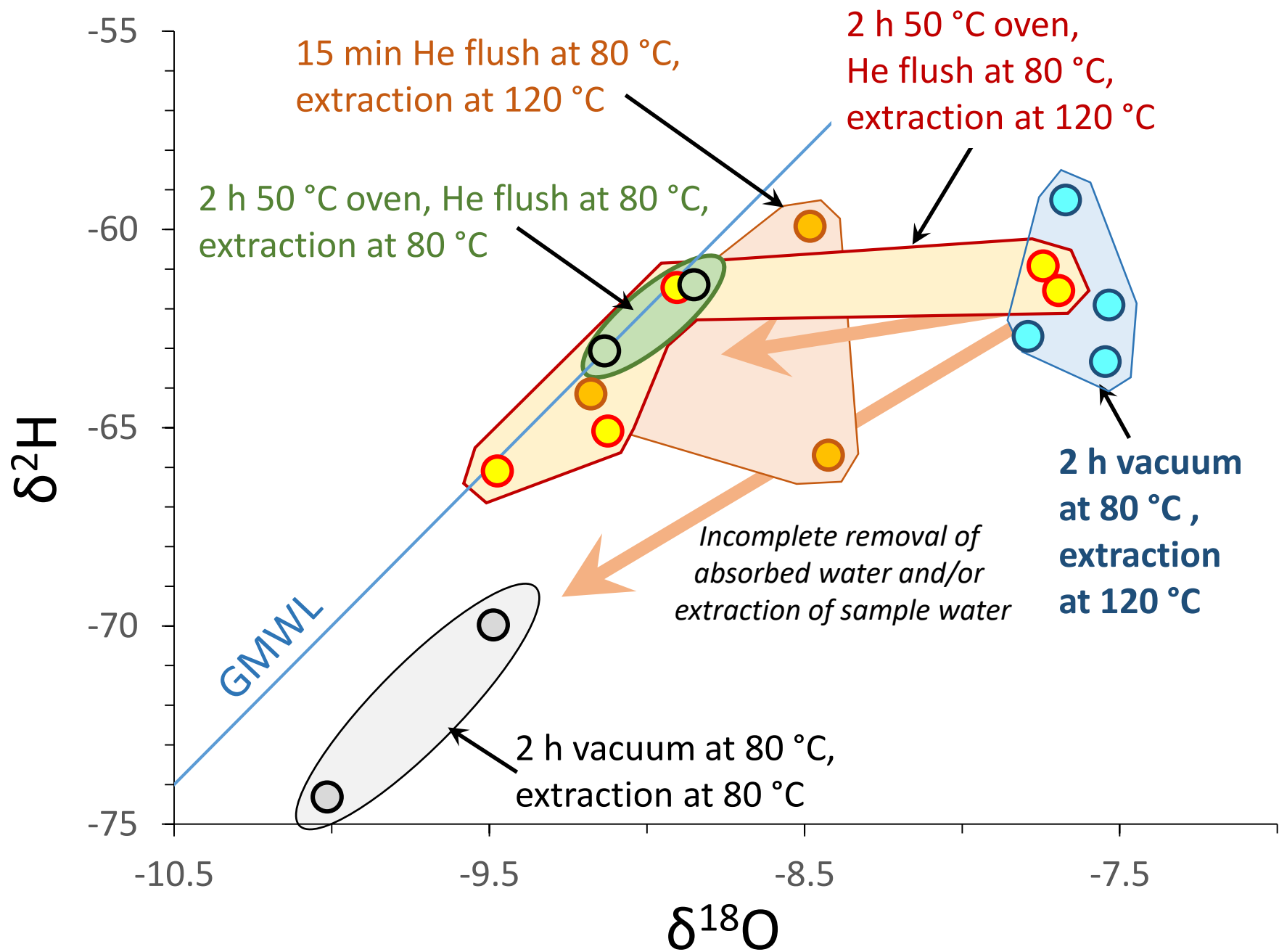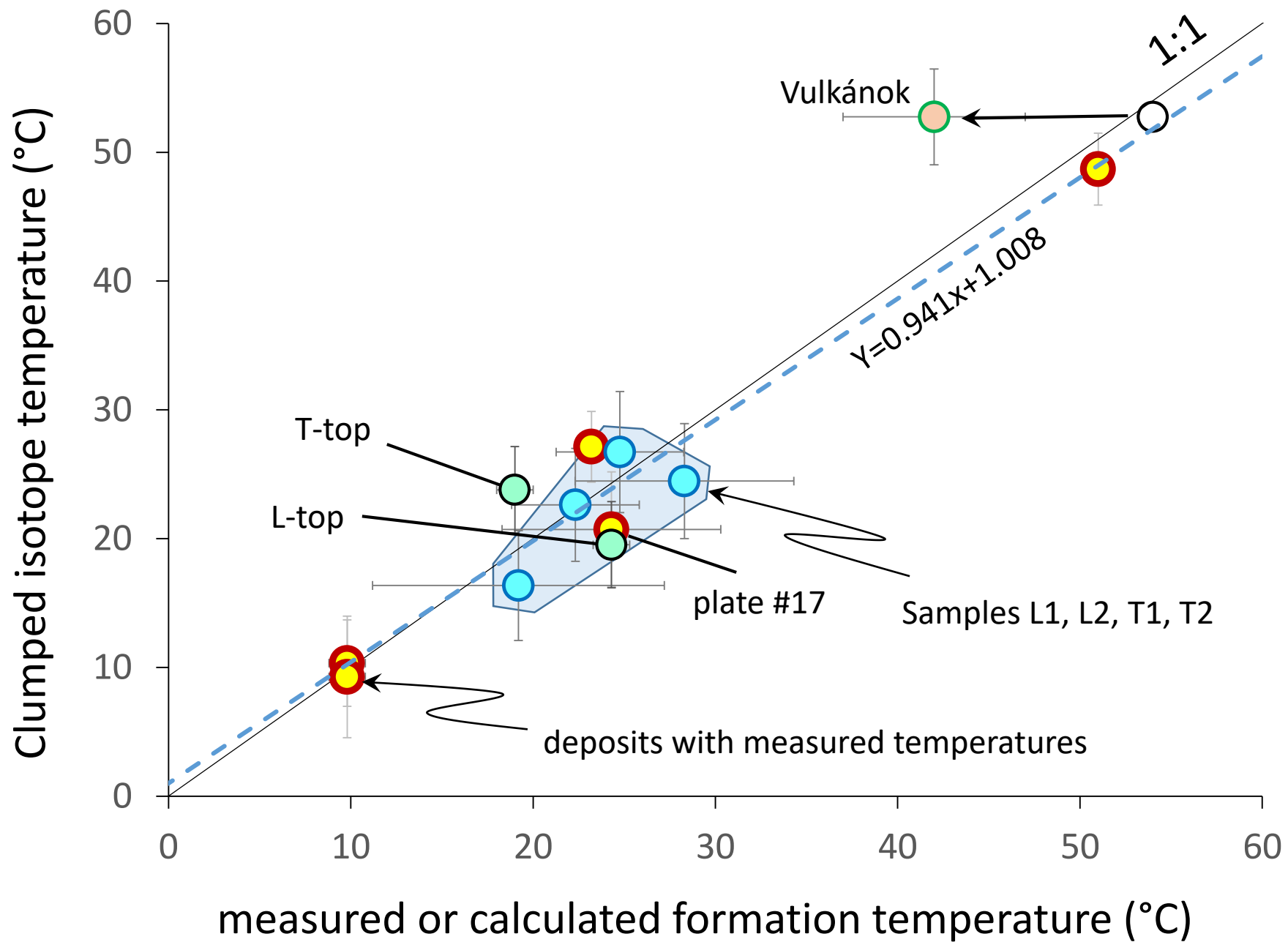
Supplementary Table 1. Stable and clumped isotope compositions of carbonates and inclusio

Sample name	δ^{13}C [VPDB, ‰]		δ^{18}O[VPDB, ‰]		Number of replicates	D47Crunch Δ_{47} [	
	Value	±1SD	Value	±1SD		Value	±1SD
M1 ("Vulkánok")	1.00	0.03	-18.19	0.09	12	0.5202	0.0162
M2 (Lukács IV)	-0.07	0.08	-15.87	0.08	12	0.5295	0.0205
M3 (calcite rafts)	-1.69	0.02	-11.71	0.03	11	0.5855	0.0190
BNT-2 top	-9.83	0.05	-6.71	0.05	11	0.6383	0.0306
BNT-2 10mm	-10.18	0.06	-6.91	0.05	8	0.6420	0.0192
Berger plate #17	-6.85	0.05	-10.86	0.08	8	0.6046	0.0443
L1	-2.28	0.06	-12.50	0.12	11	0.5867	0.0329
L2	-2.14	0.08	-11.87	0.13	12	0.5988	0.0474
T1	-2.04	0.04	-12.65	0.11	12	0.5933	0.0422
T2	-2.69	0.05	-10.80	0.11	11	0.6183	0.0393
L-Top	-5.00	0.11	-10.07	0.10	21	0.6083	0.0358
T-Top	-2.66	0.04	-10.49	0.08	21	0.5953	0.0396

…n-hosted water, as well as temperatures calculated or measured.

…l-CDES90°C, ‰]		Anderson Temp [°C]			δ^2H [VSMOW, ‰]	$\delta^{18}O$ [VSMOW, ‰]	temperature (measured or inclusion-based, °C)
±1SE	±95% CL	Value	±1SE	$\Delta(\Delta_{47})$			
0.0084	0.0166	52.7	3.7	-443.76	-86.2	-13.7	42.0 ±5
0.0083	0.0164	48.7	3.5	-427.42			51.0 ±0.5
0.0088	0.0173	27.1	3.1	-347.15			23.2 ±0.5
0.0094	0.0186	10.3	2.7	-292.07			9.8 ±0.5
0.0103	0.0205	9.3	3.0	-288.76			9.8 ±0.5
0.0145	0.0287	20.7	4.7	-325.37			24.3 ±1
0.0136	0.0267	26.7	4.7	-345.71	-72.0	-11.2	24.8 ±3.5
0.0132	0.0260	22.6	4.4	-331.74	-71.2	-11.0	22.3 ±3.5
0.0132	0.0261	24.5	4.5	-337.97	-66.7	-10.7	28.3 ±6
0.0137	0.0271	16.4	4.3	-311.10	-74.7	-10.6	19.2 ±8
0.0104	0.0205	19.5	3.3	-321.41			24.3 ±1
0.0100	0.0198	23.8	3.4	-335.68			19.0 ±1